

Analysis of Laminated Shells using Pseudospectrals and the Reissner-Mixed Variational Theorem

S. C. F. Fernandes^a, J. Cuartero^a, A. J. M. Ferreira^b,

^a*University of Zaragoza, Spain*

^b*Faculdade de Engenharia da Universidade do Porto, Portugal*

Abstract

In this paper, we combine the Carrera's Unified Formulation CUF and a pseudospectral technique for predicting the static deformations and free vibrations behaviour of thin and thick cross-ply laminated shells. For the first time, the Reissner-Mixed Variational Theorem is used together with pseudospectrals to achieve a highly accurate technique. The accuracy and efficiency of this numerical technique for static and vibration problems are demonstrated through numerical examples.

1 Introduction

The analysis of laminated shells should be performed with both an adequate shear deformation theory and a accurate numerical scheme. Shear deformations theories can be classified as equivalent single layer (ESL), where all layers are linked to the same set of degrees-of-freedom, and layerwise theories (LW) where each layer or a group of layers are linked to independent (layer-wise) degrees-of-freedom. ESL theories can be divided in first-order (such as the extension of Mindlin [1] theories for plates), or higher-order theories, such as those proposed by Pandya and Kant [2], Reddy [3] or Touratier [4]. Layerwise theories can use translational and rotational degrees-of-freedom or just translational [5].

Most of the theories use displacements as primary variables, with a post-computation procedure to obtain stresses, in particular transverse shear stresses. The Reissner-Mixed Variational Theorem (RMVT) linked with LW theories allows the direct computation of the transverse shear stresses, with the increase of computational cost, due to extra degrees-of-freedom at each layer interface.

Most of the numerical approaches so far are based on analytical solutions or the finite element solutions. More recently collocation with radial basis functions, with the so-called unsymmetrical Kansa method [6] have been presented [7,8].

In this paper we propose to combine the RMVT with a spectral collocation (also known as pseudospectral) using Chebyshev polynomials, to analyse static deformations and free vibrations of laminated doubly-curved shells. Equations of motion are in many theories time-consuming to obtain. The Unified Formulation of Carrera (also known as CUF) [9] provides a systematic procedure to derive the equations of motion and boundary conditions for laminated plates and shells, including the use of RMVT [10,9,11,12] . The same CUF technology could be applied for finite element formulation, which is not the case of the present paper.

This is the first time this formulation is discretised with pseudospectrals. Therefore, this paper contributes to fill the gap of knowledge in this research area.

2 Unified Formulation for the RMVT theory

In this section we show how we can use the Carrera's Unified formulation to obtain the fundamental nuclei, which allows the derivation of the equations of motion and boundary conditions, in its strong form for the present pseudospectral discretization.

2.1 Shell geometry

Shells are bi-dimensional structures in which one dimension (in general the thickness in z direction) is negligible with respect to the other two in-plane dimensions. Geometry and the reference system are indicated in the Figures 1 and 2. The square of an infinitesimal linear segment in the layer, the associated infinitesimal area and volume are given by:

$$\begin{aligned}
 ds_k^2 &= H_\alpha^{k2} d\alpha^2 + H_\beta^{k2} d\beta^2 + H_z^{k2} dz^2 , \\
 d\Omega_k &= H_\alpha^k H_\beta^k d\alpha d\beta , \\
 dV &= H_\alpha^k H_\beta^k H_z^k d\alpha d\beta dz ,
 \end{aligned}
 \tag{1}$$

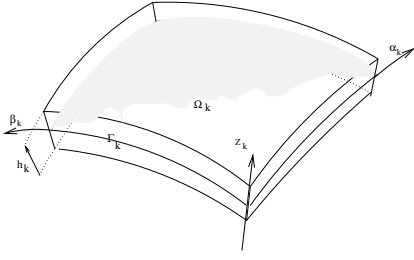


Fig. 1. Curvilinear reference system.

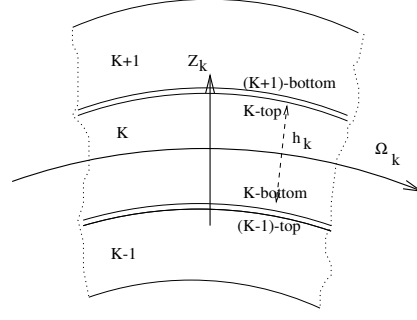


Fig. 2. Through-the-thickness reference system.

where the metric coefficients are defined as:

$$H_\alpha^k = A^k(1 + z/R_\alpha^k), \quad H_\beta^k = B^k(1 + z/R_\beta^k), \quad H_z^k = 1. \quad (2)$$

k denotes the k -layer of the multilayered shell; R_α^k and R_β^k are the principal radii of curvature along the coordinates α and β respectively. A^k and B^k are the coefficients of the first fundamental form of Ω_k (Γ_k is the Ω_k boundary). In this work, the attention has been restricted to shells with constant radii of curvature (cylindrical, spherical, toroidal geometries) for which $A^k = B^k = 1$.

3 Strains

Stresses and strains are separated into in-plane and normal components, denoted respectively by the subscripts p and n . The mechanical strains in the k th layer can be related to the displacement field $\mathbf{u}^k = \{u_\alpha^k, u_\beta^k, u_z^k\}$ via the geometrical relations:

$$\epsilon_{pG}^k = [\epsilon_{\alpha\alpha}^k, \epsilon_{\beta\beta}^k, \epsilon_{\alpha\beta}^k]^T = (\mathbf{D}_p^k + \mathbf{A}_p^k) \mathbf{u}^k, \quad \epsilon_{nG}^k = [\epsilon_{\alpha z}^k, \epsilon_{\beta z}^k, \epsilon_{zz}^k]^T = (\mathbf{D}_{n\Omega}^k + \mathbf{D}_{nz}^k - \mathbf{A}_n^k) \mathbf{u}^k \quad (3)$$

The explicit form of the introduced arrays follows:

$$\mathbf{D}_p^k = \begin{bmatrix} \frac{\partial_\alpha}{H_\alpha^k} & 0 & 0 \\ 0 & \frac{\partial_\beta}{H_\beta^k} & 0 \\ \frac{\partial_\beta}{H_\beta^k} & \frac{\partial_\alpha}{H_\alpha^k} & 0 \end{bmatrix}, \quad \mathbf{D}_{n\Omega}^k = \begin{bmatrix} 0 & 0 & \frac{\partial_\alpha}{H_\alpha^k} \\ 0 & 0 & \frac{\partial_\beta}{H_\beta^k} \\ 0 & 0 & 0 \end{bmatrix}, \quad \mathbf{D}_{nz}^k = \begin{bmatrix} \partial_z & 0 & 0 \\ 0 & \partial_z & 0 \\ 0 & 0 & \partial_z \end{bmatrix}, \quad (4)$$

$$\mathbf{A}_p^k = \begin{bmatrix} 0 & 0 & \frac{1}{H_\alpha^k R_\alpha^k} \\ 0 & 0 & \frac{1}{H_\beta^k R_\beta^k} \\ 0 & 0 & 0 \end{bmatrix}, \quad \mathbf{A}_n^k = \begin{bmatrix} \frac{1}{H_\alpha^k R_\alpha^k} & 0 & 0 \\ 0 & \frac{1}{H_\beta^k R_\beta^k} & 0 \\ 0 & 0 & 0 \end{bmatrix}. \quad (5)$$

4 Stresses

The expressions of the constitutive relations for a classical model, opportunely separated in in-plane and out-plane components state:

$$\begin{aligned}\boldsymbol{\sigma}_p^k &= \mathbf{C}_{pp}^k(z) \boldsymbol{\epsilon}_p^k + \mathbf{C}_{pn}^k(z) \boldsymbol{\epsilon}_n^k \\ \boldsymbol{\sigma}_n^k &= \mathbf{C}_{np}^k(z) \boldsymbol{\epsilon}_p^k + \mathbf{C}_{nn}^k(z) \boldsymbol{\epsilon}_n^k\end{aligned}\quad (6)$$

In case of RMVT displacements \mathbf{u} and transverse shear/normal stresses $\boldsymbol{\sigma}_n$ are both a priori variables, so constitutive equations are rewritten as:

$$\begin{aligned}\boldsymbol{\sigma}_p^k &= \tilde{\mathbf{C}}_{pp}^k(z) \boldsymbol{\epsilon}_p^k + \tilde{\mathbf{C}}_{pn}^k(z) \boldsymbol{\sigma}_n^k \\ \boldsymbol{\epsilon}_n^k &= \tilde{\mathbf{C}}_{np}^k(z) \boldsymbol{\epsilon}_p^k + \tilde{\mathbf{C}}_{nn}^k(z) \boldsymbol{\sigma}_n^k\end{aligned}\quad (7)$$

where the new coefficients are:

$$\begin{aligned}\tilde{\mathbf{C}}_{pp}^k(z) &= \mathbf{C}_{pp}^k(z) - \mathbf{C}_{pn}^k(z) \mathbf{C}_{nn}^{k-1}(z) \mathbf{C}_{np}^k(z) & \tilde{\mathbf{C}}_{pn}^k(z) &= \mathbf{C}_{pn}^k(z) \mathbf{C}_{nn}^{k-1}(z) \\ \tilde{\mathbf{C}}_{np}^k(z) &= -\mathbf{C}_{nn}^{k-1}(z) \mathbf{C}_{np}^k(z) & \tilde{\mathbf{C}}_{nn}^k(z) &= \mathbf{C}_{nn}^{k-1}(z)\end{aligned}\quad (8)$$

In case of Layer Wise (LW) models, each layer k of the given multi-layered structure is separately considered. According to the CUF, the three displacement components u , v and w and their relative variations can be modelled as:

$$(u^k, v^k, w^k) = F_\tau^k (u_\tau^k, v_\tau^k, w_\tau^k) \quad (\delta u^k, \delta v^k, \delta w^k) = F_s^k (\delta u_s^k, \delta v_s^k, \delta w_s^k) \quad (9)$$

In the present formulation, we choose:

$$F_\tau^k = \left[\frac{1 - 2/h_k \left(z - \frac{1}{2}(z_k + z_{k+1}) \right)}{2} \quad \frac{1 + 2/h_k \left(z - \frac{1}{2}(z_k + z_{k+1}) \right)}{2} \right]$$

for displacements u, v, w . Note that z_k, z_{k+1} correspond to the bottom and top z -coordinates for each layer k .

In a similar way, the transverse shear/normal stresses $\boldsymbol{\sigma}_n = (\sigma_{\alpha z}, \sigma_{\beta z}, \sigma_{zz})$ can also be modelled as

$$\boldsymbol{\sigma}_n^k = F_t \boldsymbol{\sigma}_{nt}^k + F_b \boldsymbol{\sigma}_{nb}^k = F_\tau \boldsymbol{\sigma}_\tau^k \quad (10)$$

We then obtain all terms of the equations of motion by integrating through the thickness direction.

5 Governing equations by RMVT

Taking into account the metric coefficients H_α and H_β , the Reissner's Mixed Variational Theorem is defined as:

$$\sum_{k=1}^{N_l} \int_{\Omega_k} \int_{A_k} \left\{ \delta \epsilon_{pG}^k T \sigma_{pC}^k + \delta \epsilon_{nG}^k T \sigma_{nM}^k + \delta \sigma_{nM}^k T (\epsilon_{nG}^k - \epsilon_{nC}^k) \right\} H_\alpha H_\beta d\Omega_k dz = \sum_{k=1}^{N_l} \delta L_e^k \quad (11)$$

where the meaning of the subscripts is: M = modelled a-priori, G = derived from geometrical relations and C = obtained via the constitutive equations. Substituting the geometrical relations for the shell (3), the constitutive equations (7) and the CUF for both displacement components and transverse stresses in Eq.(11), and then performing the integration by parts, the governing equations in case of RMVT are:

$$\begin{aligned} \delta \mathbf{u}_s^k T : \quad & \mathbf{K}_{uu}^{k\tau s} \mathbf{u}_\tau^k + \mathbf{K}_{u\sigma}^{k\tau s} \boldsymbol{\sigma}_{n\tau}^k = \mathbf{P}_{u\tau}^k \\ \delta \boldsymbol{\sigma}_{ns}^k T : \quad & \mathbf{K}_{\sigma u}^{k\tau s} \mathbf{u}_\tau^k + \mathbf{K}_{\sigma\sigma}^{k\tau s} \boldsymbol{\sigma}_{n\tau}^k = 0 \end{aligned} \quad (12)$$

with boundary conditions state:

$$\mathbf{\Pi}_u^{k\tau s} \mathbf{u}_\tau^k + \mathbf{\Pi}_\sigma^{k\tau s} \boldsymbol{\sigma}_{n\tau}^k = \mathbf{\Pi}_u^{k\tau s} \bar{\mathbf{u}}_\tau^k + \mathbf{\Pi}_\sigma^{k\tau s} \bar{\boldsymbol{\sigma}}_{n\tau}^k \quad (13)$$

In figure 3 it is shown the assembling procedure on layer k for the LW approach.

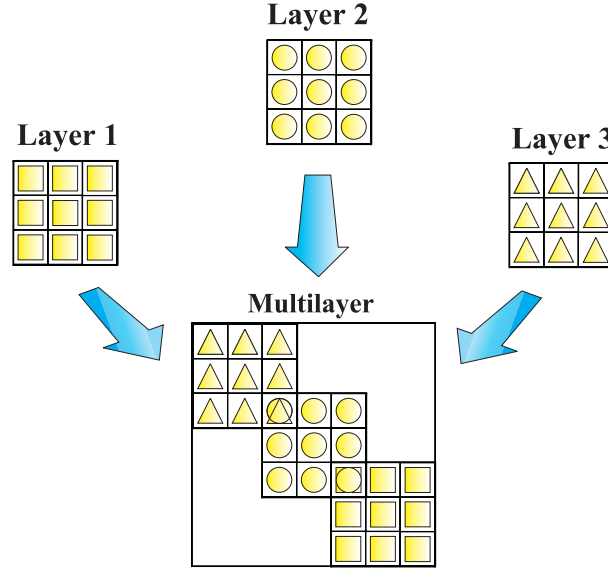


Fig. 3. Assembling procedure for LW approach.

In figure 4 it is illustrated how the degrees of freedom are defined at each

interface. It is very clear that the RMVT formulation increases the computational cost significantly. As we will show later in the paper this cost also brings excellent accuracy.

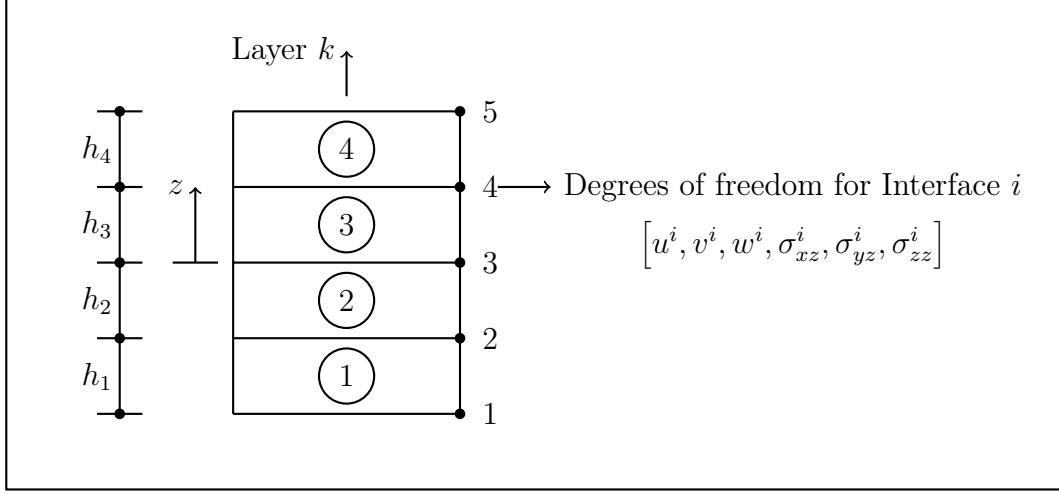


Fig. 4. A 4-layer laminate; definition of degrees of freedom at interfaces

6 Fundamental nuclei

In order to obtain the explicit terms of the expanding kernel (denoted as fundamental nuclei by Carrera), the following integrals are introduced. Such J terms will be multiplied by the materials terms for each layer, as in equation (23).

$$\begin{aligned}
(J^{k\tau s}, J_{\alpha}^{k\tau s}, J_{\beta}^{k\tau s}, J_{\frac{\alpha}{\beta}}^{k\tau s}, J_{\frac{\beta}{\alpha}}^{k\tau s}, J_{\alpha\beta}^{k\tau s}) &= \int_{A_k} F_{\tau} F_s (1, H_{\alpha}, H_{\beta}, \frac{H_{\alpha}}{H_{\beta}}, \frac{H_{\beta}}{H_{\alpha}}, H_{\alpha} H_{\beta}) dz \\
(J^{k\tau_z s}, J_{\alpha}^{k\tau_z s}, J_{\beta}^{k\tau_z s}, J_{\frac{\alpha}{\beta}}^{k\tau_z s}, J_{\frac{\beta}{\alpha}}^{k\tau_z s}, J_{\alpha\beta}^{k\tau_z s}) &= \int_{A_k} \frac{\partial F_{\tau}}{\partial z} F_s (1, H_{\alpha}, H_{\beta}, \frac{H_{\alpha}}{H_{\beta}}, \frac{H_{\beta}}{H_{\alpha}}, H_{\alpha} H_{\beta}) dz \\
(J^{k\tau s_z}, J_{\alpha}^{k\tau s_z}, J_{\beta}^{k\tau s_z}, J_{\frac{\alpha}{\beta}}^{k\tau s_z}, J_{\frac{\beta}{\alpha}}^{k\tau s_z}, J_{\alpha\beta}^{k\tau s_z}) &= \int_{A_k} F_{\tau} \frac{\partial F_s}{\partial z} (1, H_{\alpha}, H_{\beta}, \frac{H_{\alpha}}{H_{\beta}}, \frac{H_{\beta}}{H_{\alpha}}, H_{\alpha} H_{\beta}) dz \\
(J^{k\tau_z s_z}, J_{\alpha}^{k\tau_z s_z}, J_{\beta}^{k\tau_z s_z}, J_{\frac{\alpha}{\beta}}^{k\tau_z s_z}, J_{\frac{\beta}{\alpha}}^{k\tau_z s_z}, J_{\alpha\beta}^{k\tau_z s_z}) &= \int_{A_k} \frac{\partial F_{\tau}}{\partial z} \frac{\partial F_s}{\partial z} (1, H_{\alpha}, H_{\beta}, \frac{H_{\alpha}}{H_{\beta}}, \frac{H_{\beta}}{H_{\alpha}}, H_{\alpha} H_{\beta}) dz
\end{aligned} \tag{14}$$

The expression of fundamental nuclei for the left-hand side is expressed as:

$$\mathbf{K}^{k\tau s} = \begin{bmatrix} \mathbf{K}_{uu}^{k\tau s} & \mathbf{K}_{u\sigma}^{k\tau s} \\ \mathbf{K}_{\sigma u}^{k\tau s} & \mathbf{K}_{\sigma\sigma}^{k\tau s} \end{bmatrix} \tag{15}$$

where

$$\mathbf{K}_{uu}^{k\tau s} = \int_{A_k} \left[[-\mathbf{D}_p + \mathbf{A}_p]^T \hat{\mathbf{C}}_{\sigma_p \epsilon_p}^k [\mathbf{D}_p + \mathbf{A}_p] \right] F_s F_\tau H_\alpha H_\beta dz, \quad (16)$$

$$\mathbf{K}_{u\sigma}^{k\tau s} = \int_{A_k} \left[-\mathbf{D}_p + \mathbf{A}_p \right]^T \hat{\mathbf{C}}_{\sigma_p \sigma_n}^k + [-\mathbf{D}_{n\Omega} + \mathbf{D}_{nz} - \mathbf{A}_n]^T \left[F_s F_\tau H_\alpha H_\beta \right] dz, \quad (17)$$

$$\mathbf{K}_{\sigma u}^{k\tau s} = \int_{A_k} \left[[\mathbf{D}_{n\Omega} + \mathbf{D}_{nz} - \mathbf{A}_n] - \hat{\mathbf{C}}_{\epsilon_n \epsilon_p}^k [\mathbf{D}_p + \mathbf{A}_p] \right] F_s F_\tau H_\alpha H_\beta dz, \quad (18)$$

$$\mathbf{K}_{\sigma\sigma}^{k\tau s} = \int_{A_k} \left[-\hat{\mathbf{C}}_{\epsilon_n \sigma_n}^k \right] F_s F_\tau H_\alpha H_\beta dz, \quad (19)$$

and the nuclei for the boundary conditions are:

$$\mathbf{\Pi}_u^{k\tau s} = \int_{A_k} \left[\mathbf{I}_p^T \hat{\mathbf{C}}_{\sigma_p \epsilon_p}^k [\mathbf{D}_p + \mathbf{A}_p] \right] F_s F_\tau H_\alpha H_\beta dz, \quad (20)$$

$$\mathbf{\Pi}_\sigma^{k\tau s} = \int_{A_k} \left[\mathbf{I}_p^T \hat{\mathbf{C}}_{\sigma_p \sigma_n}^k + \mathbf{I}_{n\Omega}^T \right] F_s F_\tau H_\alpha H_\beta dz, \quad (21)$$

Using the notation given in equations (14), the nuclei components $\mathbf{K}_{uu}^{k\tau s}$ in explicit form are given as:

$$\mathbf{K}_{uu}^{k\tau s} = \begin{bmatrix} K_{uu11}^{k\tau s} & K_{uu12}^{k\tau s} & K_{uu13}^{k\tau s} \\ K_{uu21}^{k\tau s} & K_{uu22}^{k\tau s} & K_{uu23}^{k\tau s} \\ K_{uu31}^{k\tau s} & K_{uu32}^{k\tau s} & K_{uu33}^{k\tau s} \end{bmatrix} \quad (22)$$

where

$$\begin{aligned} K_{uu11}^{k\tau s} = & -\partial_\alpha^\tau \partial_\alpha^s C_{11}^k J_{\beta/\alpha}^{k\tau s} - \partial_\alpha^\tau \partial_\beta^s C_{16}^k J^{k\tau s} - \partial_\beta^\tau \partial_\alpha^s C_{16}^k J^{k\tau s} + \partial_\alpha^\tau \partial_\alpha^s \frac{C_{13}^{k^2}}{C_{33}^k} J_{\beta/\alpha}^{k\tau s} + \\ & \partial_\alpha^\tau \partial_\beta^s \frac{C_{13}^k C_{36}^k}{C_{33}^k} J^{k\tau s} + \partial_\beta^\tau \partial_\alpha^s \frac{C_{13}^k C_{36}^k}{C_{33}^k} J^{k\tau s} + \partial_\beta^\tau \partial_\beta^s \frac{C_{36}^{k^2}}{C_{33}^k} J_{\alpha/\beta}^{k\tau s} - \partial_\beta^\tau \partial_\beta^s C_{66}^k J_{\alpha/\beta}^{k\tau s} \end{aligned} \quad (23)$$

$$\begin{aligned}
K_{uu_{12}}^{k\tau s} &= -\partial_\alpha^\tau \partial_\beta^s C_{12}^k J^{k\tau s} - \partial_\alpha^\tau \partial_\alpha^s C_{16}^k J_{\beta/\alpha}^{k\tau s} - \partial_\beta^\tau \partial_\beta^s C_{26}^k J_{\alpha/\beta}^{k\tau s} + \partial_\alpha^\tau \partial_\beta^s \frac{C_{13}^k C_{23}^k}{C_{33}^k} J^{k\tau s} + \\
&\quad \partial_\alpha^\tau \partial_\alpha^s \frac{C_{13}^k C_{36}^k}{C_{33}^k} J_{\beta/\alpha}^{k\tau s} + \partial_\beta^\tau \partial_\beta^s \frac{C_{23}^k C_{36}^k}{C_{33}^k} J_{\alpha/\beta}^{k\tau s} + \partial_\beta^\tau \partial_\alpha^s \frac{C_{36}^{k^2}}{C_{33}^k} J^{k\tau s} - \partial_\beta^\tau \partial_\alpha^s C_{66}^k J^{k\tau s}
\end{aligned} \tag{24}$$

$$\begin{aligned}
K_{uu_{13}}^{k\tau s} &= -\frac{1}{R_\alpha^k} \partial_\beta^\tau C_{16}^k J^{k\tau s} - \frac{1}{R_\beta^k} \partial_\beta^\tau C_{26}^k J_{\alpha/\beta}^{k\tau s} + \frac{1}{R_\alpha^k} \partial_\beta^\tau \frac{C_{13}^k C_{36}^k}{C_{33}^k} J^{k\tau s} + \frac{1}{R_\beta^k} \partial_\beta^\tau \frac{C_{23}^k C_{36}^k}{C_{33}^k} J_{\alpha/\beta}^{k\tau s} - \\
&\quad \frac{1}{R_\alpha^k} \partial_\alpha^\tau C_{11}^k J_{\beta/\alpha}^{k\tau s} - \frac{1}{R_\beta^k} \partial_\alpha^\tau C_{12}^k J^{k\tau s} + \frac{1}{R_\alpha^k} \partial_\alpha^\tau \frac{C_{13}^{k^2}}{C_{33}^k} J_{\beta/\alpha}^{k\tau s} + \frac{1}{R_\beta^k} \partial_\alpha^\tau \frac{C_{13}^k C_{23}^k}{C_{33}^k} J^{k\tau s}
\end{aligned} \tag{25}$$

$$\begin{aligned}
K_{uu_{21}}^{k\tau s} &= -\partial_\beta^\tau \partial_\alpha^s C_{12}^k J^{k\tau s} - \partial_\alpha^\tau \partial_\alpha^s C_{16}^k J_{\beta/\alpha}^{k\tau s} - \partial_\beta^\tau \partial_\beta^s C_{26}^k J_{\alpha/\beta}^{k\tau s} + \partial_\beta^\tau \partial_\alpha^s \frac{C_{13}^k C_{23}^k}{C_{33}^k} J^{k\tau s} + \\
&\quad \partial_\alpha^\tau \partial_\alpha^s \frac{C_{13}^k C_{36}^k}{C_{33}^k} J_{\beta/\alpha}^{k\tau s} + \partial_\beta^\tau \partial_\beta^s \frac{C_{23}^k C_{36}^k}{C_{33}^k} J_{\alpha/\beta}^{k\tau s} + \partial_\alpha^\tau \partial_\beta^s \frac{C_{36}^{k^2}}{C_{33}^k} J^{k\tau s} - \partial_\alpha^\tau \partial_\beta^s C_{66}^k J^{k\tau s}
\end{aligned} \tag{26}$$

$$\begin{aligned}
K_{uu_{22}}^{k\tau s} &= -\partial_\beta^\tau \partial_\beta^s C_{22}^k J_{\alpha/\beta}^{k\tau s} - \partial_\alpha^\tau \partial_\beta^s C_{26}^k J^{k\tau s} - \partial_\beta^\tau \partial_\alpha^s C_{26}^k J^{k\tau s} + \partial_\beta^\tau \partial_\beta^s \frac{C_{23}^{k^2}}{C_{33}^k} J_{\alpha/\beta}^{k\tau s} + \\
&\quad \partial_\alpha^\tau \partial_\beta^s \frac{C_{23}^k C_{36}^k}{C_{33}^k} J^{k\tau s} + \partial_\beta^\tau \partial_\alpha^s \frac{C_{23}^k C_{36}^k}{C_{33}^k} J^{k\tau s} + \partial_\alpha^\tau \partial_\alpha^s \frac{C_{36}^{k^2}}{C_{33}^k} J_{\beta/\alpha}^{k\tau s} - \partial_\alpha^\tau \partial_\alpha^s C_{66}^k J_{\beta/\alpha}^{k\tau s}
\end{aligned} \tag{27}$$

$$\begin{aligned}
K_{uu_{23}}^{k\tau s} &= -\frac{1}{R_\alpha^k} \partial_\beta^\tau C_{12}^k J^{k\tau s} - \frac{1}{R_\beta^k} \partial_\beta^\tau C_{22}^k J_{\alpha/\beta}^{k\tau s} + \frac{1}{R_\alpha^k} \partial_\beta^\tau \frac{C_{13}^k C_{23}^k}{C_{33}^k} J^{k\tau s} + \frac{1}{R_\beta^k} \partial_\beta^\tau \frac{C_{23}^{k^2}}{C_{33}^k} J_{\alpha/\beta}^{k\tau s} - \\
&\quad \frac{1}{R_\alpha^k} \partial_\alpha^\tau C_{16}^k J_{\beta/\alpha}^{k\tau s} - \frac{1}{R_\beta^k} \partial_\alpha^\tau C_{26}^k J^{k\tau s} + \frac{1}{R_\alpha^k} \partial_\alpha^\tau \frac{C_{13}^k C_{36}^k}{C_{33}^k} J_{\beta/\alpha}^{k\tau s} + \frac{1}{R_\beta^k} \partial_\alpha^\tau \frac{C_{23}^k C_{36}^k}{C_{33}^k} J^{k\tau s}
\end{aligned} \tag{28}$$

$$\begin{aligned}
K_{uu_{31}}^{k\tau s} &= \frac{1}{R_\alpha^k} \partial_\beta^s C_{16}^k J^{k\tau s} + \frac{1}{R_\beta^k} \partial_\beta^s C_{26}^k J_{\alpha/\beta}^{k\tau s} - \frac{1}{R_\alpha^k} \partial_\beta^s \frac{C_{13}^k C_{36}^k}{C_{33}^k} J^{k\tau s} - \frac{1}{R_\beta^k} \partial_\beta^s \frac{C_{23}^k C_{36}^k}{C_{33}^k} J_{\alpha/\beta}^{k\tau s} + \\
&\quad \frac{1}{R_\alpha^k} \partial_\alpha^s C_{11}^k J_{\beta/\alpha}^{k\tau s} + \frac{1}{R_\beta^k} \partial_\alpha^s C_{12}^k J^{k\tau s} - \frac{1}{R_\alpha^k} \partial_\alpha^s \frac{C_{13}^{k^2}}{C_{33}^k} J_{\beta/\alpha}^{k\tau s} - \frac{1}{R_\beta^k} \partial_\alpha^s \frac{C_{13}^k C_{23}^k}{C_{33}^k} J^{k\tau s}
\end{aligned} \tag{29}$$

$$\begin{aligned}
K_{uu_{32}}^{k\tau s} &= \frac{1}{R_\alpha^k} \partial_\beta^s C_{12}^k J^{k\tau s} + \frac{1}{R_\beta^k} \partial_\beta^s C_{22}^k J_{\alpha/\beta}^{k\tau s} - \frac{1}{R_\alpha^k} \partial_\beta^s \frac{C_{13}^k C_{23}^k}{C_{33}^k} J^{k\tau s} - \frac{1}{R_\beta^k} \partial_\beta^s \frac{C_{23}^{k^2}}{C_{33}^k} J_{\alpha/\beta}^{k\tau s} + \\
&\frac{1}{R_\alpha^k} \partial_\alpha^s C_{16}^k J_{\beta/\alpha}^{k\tau s} + \frac{1}{R_\beta^k} \partial_\alpha^s C_{26}^k J^{k\tau s} - \frac{1}{R_\alpha^k} \partial_\alpha^s \frac{C_{13}^k C_{36}^k}{C_{33}^k} J_{\beta/\alpha}^{k\tau s} - \frac{1}{R_\beta^k} \partial_\alpha^s \frac{C_{23}^k C_{36}^k}{C_{33}^k} J^{k\tau s}
\end{aligned} \tag{30}$$

$$\begin{aligned}
K_{uu_{33}}^{k\tau s} &= \frac{1}{R_\alpha^{k^2}} C_{11}^k J_{\beta/\alpha}^{k\tau s} + \frac{2}{R_\alpha^k R_\beta^k} C_{12}^k J^{k\tau s} + \frac{1}{R_\beta^{k^2}} C_{22}^k J_{\alpha/\beta}^{k\tau s} - \frac{1}{R_\alpha^{k^2}} \frac{C_{13}^{k^2}}{C_{33}^k} J_{\beta/\alpha}^{k\tau s} - \\
&\frac{2}{R_\alpha^k R_\beta^k} \frac{C_{13}^k C_{23}^k}{C_{33}^k} J^{k\tau s} - \frac{1}{R_\beta^{k^2}} \frac{C_{23}^{k^2}}{C_{33}^k} J_{\alpha/\beta}^{k\tau s}
\end{aligned} \tag{31}$$

$$\begin{aligned}
\mathbf{K}_{u\sigma}^{k\tau s} &= \begin{bmatrix} K_{u\sigma_{11}}^{k\tau s} & K_{u\sigma_{12}}^{k\tau s} & K_{u\sigma_{13}}^{k\tau s} \\ K_{u\sigma_{21}}^{k\tau s} & K_{u\sigma_{22}}^{k\tau s} & K_{u\sigma_{23}}^{k\tau s} \\ K_{u\sigma_{31}}^{k\tau s} & K_{u\sigma_{32}}^{k\tau s} & K_{u\sigma_{33}}^{k\tau s} \end{bmatrix} = \\
&\left[\begin{array}{c|c|c} -\frac{1}{R_\alpha^k} J_\beta^{k\tau s} + J_{\alpha\beta}^{k\tau, z^s} & 0 & -\partial_\alpha^\tau \frac{C_{13}^k}{C_{33}^k} J_\beta^{k\tau s} - \partial_\beta^\tau \frac{C_{36}^k}{C_{33}^k} J_\alpha^{k\tau s} \\ 0 & -\frac{1}{R_\beta^k} J_\alpha^{k\tau s} + J_{\alpha\beta}^{k\tau, z^s} & -\partial_\beta^\tau \frac{C_{23}^k}{C_{33}^k} J_\alpha^{k\tau s} - \partial_\alpha^\tau \frac{C_{36}^k}{C_{33}^k} J_\beta^{k\tau s} \\ -\partial_\alpha^\tau J_\beta^{k\tau s} & -\partial_\beta^\tau J_\alpha^{k\tau s} & J_{\alpha\beta}^{k\tau, z^s} + \frac{1}{R_\alpha^k} \frac{C_{13}^k}{C_{33}^k} J_\beta^{k\tau s} + \frac{1}{R_\beta^k} \frac{C_{23}^k}{C_{33}^k} J_\alpha^{k\tau s} \end{array} \right]
\end{aligned} \tag{32}$$

$$\begin{aligned}
\mathbf{K}_{\sigma u}^{k\tau s} &= \begin{bmatrix} K_{\sigma u_{11}}^{k\tau s} & K_{\sigma u_{12}}^{k\tau s} & K_{\sigma u_{13}}^{k\tau s} \\ K_{\sigma u_{21}}^{k\tau s} & K_{\sigma u_{22}}^{k\tau s} & K_{\sigma u_{23}}^{k\tau s} \\ K_{\sigma u_{31}}^{k\tau s} & K_{\sigma u_{32}}^{k\tau s} & K_{\sigma u_{33}}^{k\tau s} \end{bmatrix} = \\
&\left[\begin{array}{c|c|c} -\frac{1}{R_\alpha^k} J_\beta^{k\tau s} + J_{\alpha\beta}^{k\tau, z^s} & 0 & \partial_\alpha^s J_\beta^{k\tau s} \\ 0 & -\frac{1}{R_\beta^k} J_\alpha^{k\tau s} + J_{\alpha\beta}^{k\tau, z^s} & \partial_\beta^s J_\alpha^{k\tau s} \\ \partial_\alpha^s \frac{C_{13}^k}{C_{33}^k} J_\beta^{k\tau s} + \partial_\beta^s \frac{C_{36}^k}{C_{33}^k} J_\alpha^{k\tau s} & \partial_\beta^s \frac{C_{23}^k}{C_{33}^k} J_\alpha^{k\tau s} + \partial_\alpha^s \frac{C_{36}^k}{C_{33}^k} J_\beta^{k\tau s} & J_{\alpha\beta}^{k\tau, z^s} + \frac{1}{R_\alpha^k} \frac{C_{13}^k}{C_{33}^k} J_\beta^{k\tau s} + \frac{1}{R_\beta^k} \frac{C_{23}^k}{C_{33}^k} J_\alpha^{k\tau s} \end{array} \right]
\end{aligned} \tag{33}$$

$$\mathbf{K}_{\sigma\sigma}^{k\tau s} = \begin{bmatrix} K_{\sigma\sigma 11}^{k\tau s} & K_{\sigma\sigma 12}^{k\tau s} & K_{\sigma\sigma 13}^{k\tau s} \\ K_{\sigma\sigma 21}^{k\tau s} & K_{\sigma\sigma 22}^{k\tau s} & K_{\sigma\sigma 23}^{k\tau s} \\ K_{\sigma\sigma 31}^{k\tau s} & K_{\sigma\sigma 32}^{k\tau s} & K_{\sigma\sigma 33}^{k\tau s} \end{bmatrix} = \begin{bmatrix} \frac{C_{44}^k}{C_{45}^{k^2} - C_{44}^k C_{55}^k} J_{\alpha\beta}^{k\tau s} & \frac{C_{45}^k}{-C_{45}^{k^2} + C_{44}^k C_{55}^k} J_{\alpha\beta}^{k\tau s} & 0 \\ \frac{C_{45}^k}{-C_{45}^{k^2} + C_{44}^k C_{55}^k} J_{\alpha\beta}^{k\tau s} & \frac{C_{55}^k}{C_{45}^{k^2} - C_{44}^k C_{55}^k} J_{\alpha\beta}^{k\tau s} & 0 \\ 0 & 0 & -\frac{1}{C_{33}^k} J_{\alpha\beta}^{k\tau s} \end{bmatrix} \quad (34)$$

7 Interpolation with pseudospectrals

We give now a short description of how we perform computations in MATLAB, inspired by Trefethen's book [13]. First we define geometry of the square plate from -1 to +1, as

```
% % definition of grid points
x = cos(pi*(0:N)/N)';
y = x; [xx,yy] = meshgrid(x,y); xx = xx(:); yy = yy(:);
NN=(N+1)^2; I = eye(N+1);
points = [xx(:) yy(:)];
```

Then we call the routine `cheb.m` in [13] to create the Chebyshev differentiation matrix and the derivatives using Kronecker products:

```
[D,x] = cheb(N); D2 = D^2;
Dy=kron(D,I); Dx=kron(I,D);
Dxx=kron(I,D2);
Dyy=kron(D2,I);
Dxy=Dx*Dy;
```

At each equation of motion, we now replace analytical derivatives by differentiation matrices. For example in equation (35)

$$\begin{aligned} K_{uu_{11}}^{k\tau s} = & -\partial_\alpha^\tau \partial_\alpha^s C_{11}^k J_{\beta/\alpha}^{k\tau s} - \partial_\alpha^\tau \partial_\beta^s C_{16}^k J^{k\tau s} - \partial_\beta^\tau \partial_\alpha^s C_{16}^k J^{k\tau s} + \partial_\alpha^\tau \partial_\alpha^s \frac{C_{13}^{k^2}}{C_{33}^k} J_{\beta/\alpha}^{k\tau s} + \\ & \partial_\alpha^\tau \partial_\beta^s \frac{C_{13}^k C_{36}^k}{C_{33}^k} J^{k\tau s} + \partial_\beta^\tau \partial_\alpha^s \frac{C_{13}^k C_{36}^k}{C_{33}^k} J^{k\tau s} + \partial_\beta^\tau \partial_\beta^s \frac{C_{36}^{k^2}}{C_{33}^k} J_{\alpha/\beta}^{k\tau s} - \partial_\beta^\tau \partial_\beta^s C_{66}^k J_{\alpha/\beta}^{k\tau s} \end{aligned} \quad (35)$$

such differential operators will be coded in MATLAB as

$$\begin{aligned}
\text{Kuu}(i1:i2,j1:j2) = & \text{Kuu}(i1:i2,j1:j2) - c11 * \text{JBetaOverAlpha}(i,j) * \text{Dxx} \dots \\
& - 2 * c16 * J1(i,j) * \text{Dxy} \dots \\
& + c13^2 / c33 * \text{JBetaOverAlpha}(i,j) * \text{Dxx} \dots \\
& + 2 * c13 * c36 / c33 * J1(i,j) * \text{Dxy} \dots \\
& + c36^2 / c33 * \text{JAlphaOverBeta}(i,j) * \text{Dyy} \dots \\
& - c66 * \text{JAlphaOverBeta}(i,j) * \text{Dyy};
\end{aligned}$$

Here, Dxx represents a $(N + 1)^2$ matrix containing the second derivatives to α : $\partial_\alpha^\tau \partial_\alpha^s$.

8 Boundary conditions

The natural boundary conditions can be applied by computing firstly the matrix

$$\mathbf{\Pi}_{uu}^{k\tau s} = \begin{bmatrix} \Pi_{uu11}^{k\tau s} & \Pi_{uu12}^{k\tau s} & \Pi_{uu13}^{k\tau s} \\ \Pi_{uu21}^{k\tau s} & \Pi_{uu22}^{k\tau s} & \Pi_{uu23}^{k\tau s} \\ \Pi_{uu31}^{k\tau s} & \Pi_{uu32}^{k\tau s} & \Pi_{uu33}^{k\tau s} \end{bmatrix} \quad (36)$$

$$\begin{aligned}
\Pi_{uu11}^{k\tau s} = & n_\alpha \partial_\alpha^s C_{11}^k J_{\beta/\alpha}^{k\tau s} + n_\alpha \partial_\beta^s C_{16}^k J^{k\tau s} + n_\beta \partial_\alpha^s C_{16}^k J^{k\tau s} - n_\alpha \partial_\alpha^s \frac{C_{13}^{k^2}}{C_{33}} J_{\beta/\alpha}^{k\tau s} - \\
& n_\alpha \partial_\beta^s \frac{C_{13}^k C_{36}^k}{C_{33}^k} J^{k\tau s} - n_\beta \partial_\alpha^s \frac{C_{13}^k C_{36}^k}{C_{33}^k} J^{k\tau s} - n_\beta \partial_\beta^s \frac{C_{36}^{k^2}}{C_{33}^k} J_{\alpha/\beta}^{k\tau s} + n_\beta \partial_\beta^s C_{66}^k J_{\alpha/\beta}^{k\tau s}
\end{aligned} \quad (37)$$

$$\begin{aligned}
\Pi_{uu12}^{k\tau s} = & n_\alpha \partial_\beta^s C_{12}^k J^{k\tau s} + n_\alpha \partial_\alpha^s C_{16}^k J_{\beta/\alpha}^{k\tau s} + n_\beta \partial_\beta^s C_{26}^k J_{\alpha/\beta}^{k\tau s} - n_\alpha \partial_\beta^s \frac{C_{13}^k C_{23}^k}{C_{33}^k} J^{k\tau s} - \\
& n_\alpha \partial_\alpha^s \frac{C_{13}^k C_{36}^k}{C_{33}^k} J_{\beta/\alpha}^{k\tau s} - n_\beta \partial_\beta^s \frac{C_{23}^k C_{36}^k}{C_{33}^k} J_{\alpha/\beta}^{k\tau s} - n_\beta \partial_\alpha^s \frac{C_{36}^{k^2}}{C_{33}^k} J^{k\tau s} + n_\beta \partial_\alpha^s C_{66}^k J^{k\tau s}
\end{aligned} \quad (38)$$

$$\begin{aligned}
\Pi_{uu_{13}}^{k\tau s} &= \frac{1}{R_\alpha^k} n_\beta C_{16}^k J^{k\tau s} + \frac{1}{R_\beta^k} n_\beta C_{26}^k J_{\alpha/\beta}^{k\tau s} - \frac{1}{R_\alpha^k} n_\beta \frac{C_{13}^k C_{36}^k}{C_{33}^k} J^{k\tau s} - \frac{1}{R_\beta^k} n_\beta \frac{C_{23}^k C_{36}^k}{C_{33}^k} J_{\alpha/\beta}^{k\tau s} + \\
&\frac{1}{R_\alpha^k} n_\alpha C_{11}^k J_{\beta/\alpha}^{k\tau s} + \frac{1}{R_\beta^k} n_\alpha C_{12}^k J^{k\tau s} - \frac{1}{R_\alpha^k} n_\alpha \frac{C_{13}^{k^2}}{C_{33}^k} J_{\beta/\alpha}^{k\tau s} - \frac{1}{R_\beta^k} n_\alpha \frac{C_{13}^k C_{23}^k}{C_{33}^k} J^{k\tau s}
\end{aligned} \tag{39}$$

$$\begin{aligned}
\Pi_{uu_{21}}^{k\tau s} &= n_\beta \partial_\alpha^s C_{12}^k J^{k\tau s} + n_\alpha \partial_\alpha^s C_{16}^k J_{\beta/\alpha}^{k\tau s} + n_\beta \partial_\beta^s C_{26}^k J_{\alpha/\beta}^{k\tau s} - n_\beta \partial_\alpha^s \frac{C_{13}^k C_{23}^k}{C_{33}^k} J^{k\tau s} - \\
&n_\alpha \partial_\alpha^s \frac{C_{13}^k C_{36}^k}{C_{33}^k} J_{\beta/\alpha}^{k\tau s} - n_\beta \partial_\beta^s \frac{C_{23}^k C_{36}^k}{C_{33}^k} J_{\alpha/\beta}^{k\tau s} - n_\alpha \partial_\beta^s \frac{C_{36}^{k^2}}{C_{33}^k} J^{k\tau s} + n_\alpha \partial_\beta^s C_{66}^k J^{k\tau s}
\end{aligned} \tag{40}$$

$$\begin{aligned}
\Pi_{uu_{22}}^{k\tau s} &= n_\beta \partial_\beta^s C_{22}^k J_{\alpha/\beta}^{k\tau s} + n_\alpha \partial_\beta^s C_{26}^k J^{k\tau s} + n_\beta \partial_\alpha^s C_{26}^k J^{k\tau s} - n_\beta \partial_\beta^s \frac{C_{23}^{k^2}}{C_{33}^k} J_{\alpha/\beta}^{k\tau s} - \\
&n_\alpha \partial_\beta^s \frac{C_{23}^k C_{36}^k}{C_{33}^k} J^{k\tau s} - n_\beta \partial_\alpha^s \frac{C_{23}^k C_{36}^k}{C_{33}^k} J^{k\tau s} - n_\alpha \partial_\alpha^s \frac{C_{36}^{k^2}}{C_{33}^k} J_{\beta/\alpha}^{k\tau s} + n_\alpha \partial_\alpha^s C_{66}^k J_{\beta/\alpha}^{k\tau s}
\end{aligned} \tag{41}$$

$$\begin{aligned}
\Pi_{uu_{23}}^{k\tau s} &= \frac{1}{R_\alpha^k} n_\beta C_{12}^k J^{k\tau s} + \frac{1}{R_\beta^k} n_\beta C_{22}^k J_{\alpha/\beta}^{k\tau s} - \frac{1}{R_\alpha^k} n_\beta \frac{C_{13}^k C_{23}^k}{C_{33}^k} J^{k\tau s} - \frac{1}{R_\beta^k} n_\beta \frac{C_{23}^{k^2}}{C_{33}^k} J_{\alpha/\beta}^{k\tau s} + \\
&\frac{1}{R_\alpha^k} n_\alpha C_{16}^k J_{\beta/\alpha}^{k\tau s} + \frac{1}{R_\beta^k} n_\alpha C_{26}^k J^{k\tau s} - \frac{1}{R_\alpha^k} n_\alpha \frac{C_{13}^k C_{36}^k}{C_{33}^k} J_{\beta/\alpha}^{k\tau s} - \frac{1}{R_\beta^k} n_\alpha \frac{C_{23}^k C_{36}^k}{C_{33}^k} J^{k\tau s}
\end{aligned} \tag{42}$$

$$\Pi_{uu_{31}}^{k\tau s} = 0 \tag{43}$$

$$\Pi_{uu_{32}}^{k\tau s} = 0 \tag{44}$$

$$\Pi_{uu_{33}}^{k\tau s} = 0 \tag{45}$$

In a similar way, we can impose boundary conditions in terms of the transverse stresses as

$$\begin{aligned}
\Pi_{\sigma_{11}}^{k\tau s} = 0; \quad \Pi_{\sigma_{12}}^{k\tau s} = 0; \quad \Pi_{\sigma_{13}}^{k\tau s} &= n_\alpha \frac{C_{13}^k}{C_{33}^k} J_\beta^{k\tau s} + n_\beta \frac{C_{36}^k}{C_{33}^k} J_\alpha^{k\tau s} \\
\Pi_{\sigma_{21}}^{k\tau s} = 0; \quad \Pi_{\sigma_{22}}^{k\tau s} = 0; \quad \Pi_{\sigma_{23}}^{k\tau s} &= n_\beta \frac{C_{23}^k}{C_{33}^k} J_\alpha^{k\tau s} + n_\alpha \frac{C_{36}^k}{C_{33}^k} J_\beta^{k\tau s} \\
\Pi_{\sigma_{31}}^{k\tau s} &= n_\alpha J_\beta^{k\tau s}; \quad \Pi_{\sigma_{32}}^{k\tau s} = n_\beta J_\alpha^{k\tau s}; \quad \Pi_{\sigma_{33}}^{k\tau s} = 0 \quad (46)
\end{aligned}$$

9 Extension to the dynamical problem

The dynamic problem is expressed as:

$$\begin{aligned}
&\sum_{k=1}^{N_l} \int_{\Omega_k} \int_{A_k} \left\{ \delta \boldsymbol{\epsilon}_{pG}^{kT} \boldsymbol{\sigma}_{pC}^k + \delta \boldsymbol{\epsilon}_{nG}^{kT} \boldsymbol{\sigma}_{nM}^k + \delta \boldsymbol{\sigma}_{nM}^{kT} (\boldsymbol{\epsilon}_{nG}^k - \boldsymbol{\epsilon}_{nC}^k) \right\} H_\alpha H_\beta d\Omega_k dz = \\
&\sum_{k=1}^{N_l} \int_{\Omega_k} \int_{A_k} \rho^k \delta \mathbf{u}^{kT} \ddot{\mathbf{u}}^k H_\alpha H_\beta d\Omega_k dz + \sum_{k=1}^{N_l} \delta L_e^k \quad (47)
\end{aligned}$$

where ρ^k is the mass density of the k -th layer and double dots denote acceleration.

By substituting the geometrical relations, the constitutive equations and the Unified Formulation, we obtain the following governing equations:

$$\delta \mathbf{u}_s^{kT} : \quad \mathbf{K}_{uu}^{*k\tau s} \mathbf{u}_\tau^k = \mathbf{M}^{k\tau s} \ddot{\mathbf{u}}_\tau^k + \mathbf{P}_{u\tau}^k \quad (48)$$

In the case of free vibrations one has:

$$\delta \mathbf{u}_s^{kT} : \quad \mathbf{K}_{uu}^{*k\tau s} \mathbf{u}_\tau^k = \mathbf{M}^{k\tau s} \ddot{\mathbf{u}}_\tau^k \quad (49)$$

where $\mathbf{K}_{uu}^{*k\tau s} = \mathbf{K}_{uu}^{k\tau s} - \mathbf{K}_{u\sigma}^{k\tau s} [\mathbf{K}_{\sigma\sigma}^{k\tau s}]^{-1} \mathbf{K}_{\sigma u}^{k\tau s}$ and it is obtained after a static condensation procedure.

$\mathbf{M}^{k\tau s}$ is the fundamental nucleus for the inertial term. The explicit form of that is:

$$M_{11}^{k\tau s} = \rho^k F_\tau F_s; \quad M_{12}^{k\tau s} = 0; \quad M_{13}^{k\tau s} = 0 \quad (50)$$

$$M_{21}^{k\tau s} = 0; \quad M_{22}^{k\tau s} = \rho^k F_\tau F_s; \quad M_{23}^{k\tau s} = 0 \quad (51)$$

$$M_{31}^{k\tau s} = 0; \quad M_{32}^{k\tau s} = 0; \quad M_{33}^{k\tau s} = \rho^k F_\tau F_s \quad (52)$$

The boundary conditions are imposed by modification of the line j corresponding to a degree-of-freedom j . For example to impose $K_{uu} = 0$ all around the plate, we modify the K big matrix as:

```
b=find(abs(xx)==max(xx));bb=size(b,1);
f(b+11*NN)=0.0;
Kuu(b,:)=zeros(bb,12*NN);
```

First we detect the nodes at the boundary using function `find` and then we zero the right-hand side `f`, and the lines `b`. We then place the value 1 at the main diagonal using `eye`.

10 Computation of stresses

Taking into account the large number of degrees of freedom per node, the solution of the static problem is obtained after a static condensation procedure as follows. Consider the global system of equations (after imposing boundary conditions):

$$\begin{bmatrix} \mathbf{K}_{uu} & \mathbf{K}_{u\sigma} \\ \mathbf{K}_{\sigma u} & \mathbf{K}_{\sigma\sigma} \end{bmatrix} \begin{bmatrix} \mathbf{u} \\ \boldsymbol{\sigma} \end{bmatrix} = \begin{bmatrix} \mathbf{f} \\ \mathbf{0} \end{bmatrix} \quad (53)$$

The problem is reduced to

$$\mathbf{K}^*_{uu} \mathbf{u} = \mathbf{f} \quad (54)$$

where $\mathbf{K}^*_{uu} = \mathbf{K}_{uu} - \mathbf{K}_{u\sigma}[\mathbf{K}_{\sigma\sigma}]^{-1}\mathbf{K}_{\sigma u}$. After computation of the solution, transverse stresses are readily computed at each interface by

$$\boldsymbol{\sigma} = [\mathbf{K}_{\sigma\sigma}]^{-1} (-\mathbf{K}_{\sigma u} \mathbf{u}) \quad (55)$$

11 The pseudospectral method

Pseudospectral (PS) methods ([13]) are known as highly accurate solvers for PDEs, where the spatial part of the approximate solution u^h of a given PDE is represented by a linear combination of some basis functions $\phi_j, j = 1, \dots, N$,

i.e.,

$$u^h(x) = \sum_{j=1}^N c_j \phi_j(x), \quad x \in \mathbb{R} \quad (56)$$

Usually polynomial basis functions (such as Chebyshev polynomials) are used in this type of approach which leads to the limitation of tensor-product grids in higher spatial dimensions.

An important feature of pseudospectral methods is the fact that one usually is content with obtaining an approximation to the solution on a discrete set of grid points x_i , $i = 1, \dots, N$ instead of at an arbitrary point x . One of several ways to implement the pseudospectral method is via so-called differentiation matrices, i.e., one finds a matrix D such that at the grid points x_i we have $\mathbf{u}' = D\mathbf{u}$. Here $\mathbf{u} = [u^h(x_1), \dots, u^h(x_N)]^T$ is the vector of values of u^h at the grid points. Consider the expansion (56) and let $\phi_j, j = 1, \dots, N$, be an arbitrary linearly independent set of smooth functions that will serve as our basis functions. To keep the discussion as simple as possible we limit the following derivation to the univariate case. In order to obtain a formulation for the differentiation matrix D of (57) we evaluate (56) at the grid points $x_i, i = 1, \dots, N$. This results in

$$u^h(x_i) = \sum_{j=1}^N c_j \phi_j(x_i), \quad i = 1, \dots, N \quad (57)$$

or in matrix-vector notation

$$\mathbf{u} = A\mathbf{c} \quad (58)$$

where $\mathbf{c} = [c_1, \dots, c_N]^T$ is the coefficient vector, the evaluation matrix A has entries $A_{ij} = \phi_j(x_i)$, and \mathbf{u} is as before. By linearity we can also use the expansion (56) to compute the derivative of u^h by differentiating the basis functions, i.e.,

$$\frac{d}{dx} u^h(x) = \sum_{j=1}^N c_j \frac{d}{dx} \phi_j(x) \quad (59)$$

If we again evaluate at the grid points x_i then we get in matrix-vector notation

$$\mathbf{u}' = A_x \mathbf{c} \quad (60)$$

where \mathbf{u} and \mathbf{c} are as above, and the matrix A_x has entries $\frac{d}{dx} \phi_j(x_i)$.

This univariate discrete first-order differential operator is used in Trefethen's book [13] to represent also univariate higher-order operators as well as multivariate operators (as long as the underlying rectangular grid is obtained as a tensor-product of univariate grids). We follow this approach in some of our numerical examples below, by using the standard polynomial differentiation matrix based on Chebyshev polynomials.

12 Numerical examples

12.1 Spherical shell in bending

A laminated composite spherical shell is here considered, of side a and thickness h , composed of equal thickness layers oriented at $[0^\circ/90^\circ/90^\circ/0^\circ]$ and at $[0^\circ/90^\circ/0^\circ]$. The shell is subjected to a sinusoidal vertical pressure of the form

$$p_z = P \sin\left(\frac{\pi x}{a}\right) \sin\left(\frac{\pi y}{a}\right)$$

with the origin of the coordinate system located at the lower left corner on the midplane and P the maximum load (at center of shell).

The orthotropic material properties for each layer are given by

$$E_1 = 25.0E_2 \quad G_{12} = G_{13} = 0.5E_2 \quad G_{23} = 0.2E_2 \quad \nu_{12} = 0.25$$

The transverse displacements are presented in normalized form as $\bar{w} = \frac{10^3 w_{(a/2, a/2, 0)} h^3 E_2}{Pa^4}$.

The shell is simply-supported on all edges.

In table 1, an assessment of the present model is presented for the plate case ($R \rightarrow \infty$). We compare the deflections obtained with the pseudospectral method with the LW analytical solution given in [12] and the results obtained with two different shell finite elements: MITC4 and MITC9. These elements are based on CUF and they are described in details in [14]. Various thickness ratios and laminations are considered. In all the cases, the table shows that the present method is in good agreement with the FEM solution.

In table 2 we compare the static deflections for the present shell model with results of Reddy shell formulation using first-order and third-order shear-deformation theories [3] and the LW analytical solution given in [12]. We consider nodal grids with 11×11 , 13×13 , 17×17 , and 21×21 points. We consider various values of R/a and two values of a/h (10 and 100). Results

are in good agreement for various a/h ratios with the higher-order results of Reddy and the LW analytical solution.

In figure 5 it is illustrated the deformed shape of the plate discretised with 21×21 points, before adimensionalisation.

	Method	$a/h = 10$	$a/h = 100$
[0°/90°/0°]	LW [12]	7.4095	4.3400
	present (13 × 13)	7.3978	4.3062
	present (17 × 17)	7.3978	4.3062
	present (21 × 21)	7.3978	4.3062
	MITC4 (13 × 13)	7.2955	4.2573
	MITC4 (17 × 17)	7.3427	4.2915
	MITC4 (21 × 21)	7.3657	4.3082
	MITC9 (5 × 5)	7.4067	4.3375
	MITC9 (9 × 9)	7.4092	4.3397
	MITC9 (13 × 13)	7.4095	4.3399
[0°/90°/90°/0°]	LW [12]	7.3148	4.3420
	present (13 × 13)	7.3544	4.3054
	present (17 × 17)	7.3544	4.3054
	present (21 × 21)	7.3544	4.3054
	MITC4 (13 × 13)	7.2011	4.2593
	MITC4 (17 × 17)	7.2482	4.2935
	MITC4 (21 × 21)	7.2711	4.3102
	MITC9 (5 × 5)	7.3120	4.3396
	MITC9 (9 × 9)	7.3145	4.3418
	MITC9 (13 × 13)	7.3147	4.3420

Table 1

Non-dimensional central deflection, $\bar{w} = w \frac{10^3 E_2 h^3}{P_0 a^4}$ for [0°/90°/90°/0°] cross-ply laminated plate.

In figure 6 it is illustrated the evolution of the transverse shear stresses τ_{xz} , for $a/h = 10$, laminate [0/90/90]. As can be seen, the formulation does not produce zero top and bottom shear stresses, for two reasons. First, the formulation is not based on C^1 definition of transverse displacement, and second the

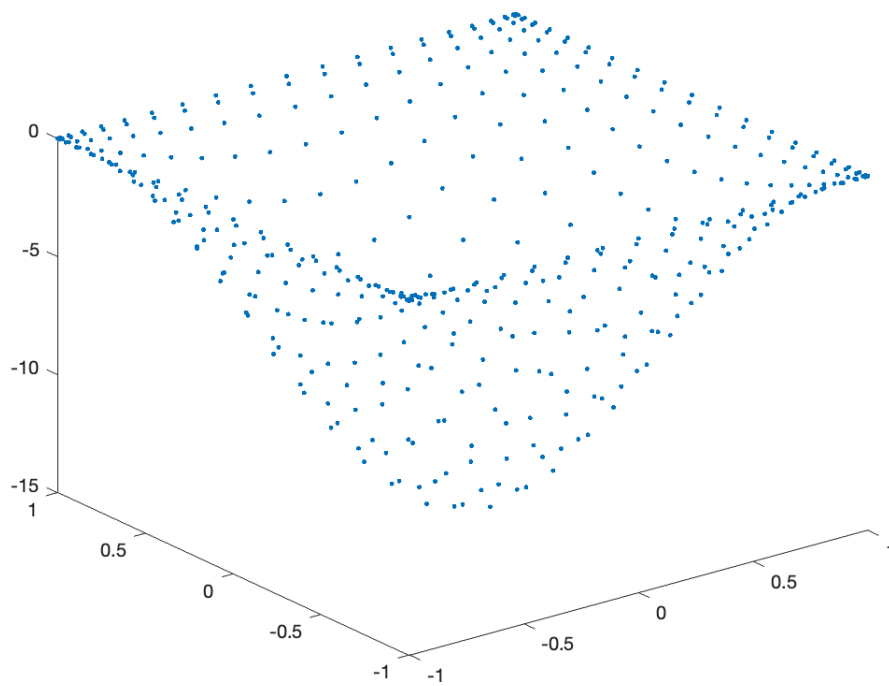


Fig. 5. Deformed shape of the $[0^\circ/90^\circ/90^\circ/0^\circ]$ cross-ply laminated plate discretised with 21×21 points, before adimensionalisation

load is not applied at the middle surface, but at the top surface. As can also be seen, because of the mixed formulation, and consideration of transverse stress variables at each interface, the transverse stresses are continuous at the laminate interfaces.

In figure 7 it is illustrated the evolution of the normal stresses σ_{xx} , for $a/h = 10$, laminate $[0/90/90]$. In both figures, a Chebyshev 17×17 grid was considered.

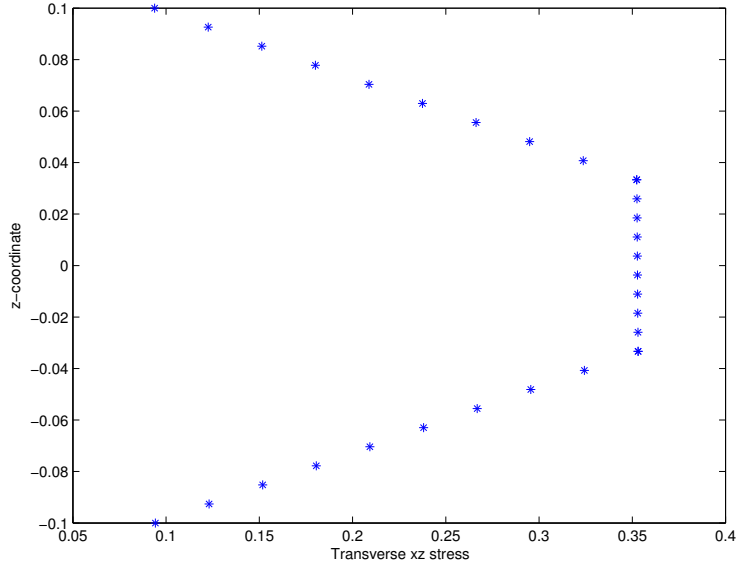


Fig. 6. Evolution of the transverse shear stresses τ_{xz} , for $a/h = 10$, laminate $[0/90/90]$.

12.2 Free vibration of spherical and cylindrical laminated shells

We consider nodal grids with 13×13 , 17×17 , and 21×21 points. In tables 3 and 4 we compare the nondimensionalized natural frequencies from the present layerwise theory for various cross-ply spherical shells, with analytical solutions by Reddy and Liu [3] who considered both the first-order (FSDT) and the third-order (HSDT) theories. The first-order theory overpredicts the fundamental natural frequencies of symmetric thick shells and symmetric shallow thin shells. The present pseudospectral method is compared with analytical results by Reddy [3] and shows excellent agreement.

Table 5 contain nondimensionalized natural frequencies obtained using the the present layerwise theory for cross-ply cylindrical shells with lamination schemes $[0/90/0]$, $[0/90/90/0]$. Present results are compared with analytical solutions by Reddy and Liu [3] who considered both the first-order (FSDT)

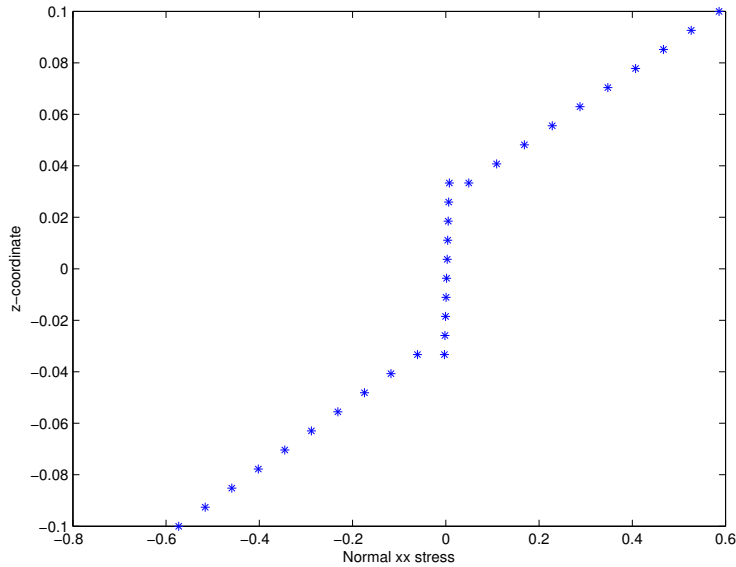


Fig. 7. Evolution of the normal stresses σ_{xx} , for $a/h = 10$, laminate [0/90/90].

and the third-order (HSDT) theories. The present method is compared with analytical results by Reddy [3] and shows excellent agreement, even with a small number of points.

13 Concluding remarks

In this paper a Reissner Mixed Variational Theorem was implemented for the first time for laminated orthotropic elastic shells through a pseudospectral discretization of equations of motion and boundary conditions. Results for static deformations and natural frequencies were obtained and compared with other sources. This meshless approach demonstrated that is very successful in the static deformations and free vibration analysis of laminated composite shells. Advantages of the pseudospectral interpolation are absence of mesh, ease of discretization of boundary conditions and equations of equilibrium or motion and very easy coding. We show that the static displacements and stresses and the natural frequencies obtained from present method are in excellent agreement with analytical or reference solutions.

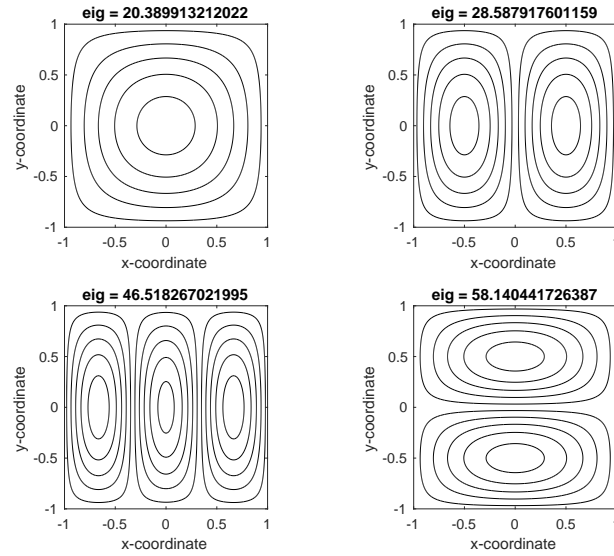


Fig. 8. First 4 vibrational modes of cross-ply laminated spherical shells, $\bar{\omega} = \omega \frac{a^2}{h} \sqrt{\rho/E_2}$, laminate $([0^\circ/90^\circ/90^\circ/0^\circ])$ grid 13×13 points, $a/h = 100, R/a = 10$

References

- [1] R. D. Mindlin. Influence of rotary inertia and shear in flexural motions of isotropic elastic plates. *Journal of Applied mechanics*, 18:31–38, 1951.
- [2] B. N. Pandya and T. Kant. Higher-order shear deformable theories for flexure of sandwich plates-finite element evaluations. *International Journal of Solids and Structures*, 24:419–451, 1988.
- [3] J. N. Reddy and C. F. Liu. A higher-order shear deformation theory of laminated

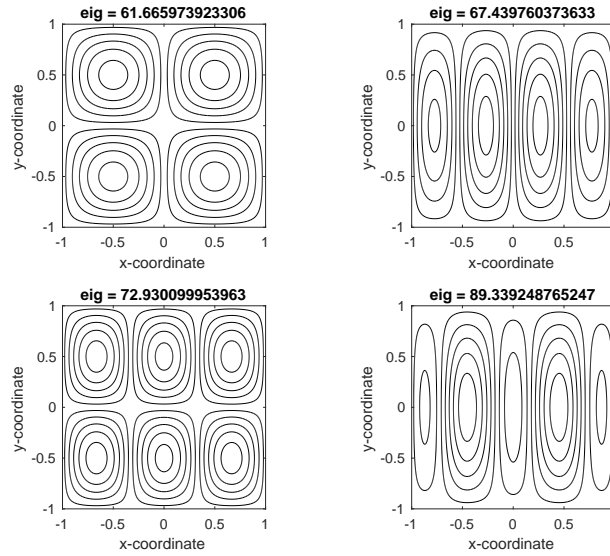


Fig. 9. Fifth to eighth vibrational modes of cross-ply laminated spherical shells, $\bar{\omega} = \omega \frac{a^2}{h} \sqrt{\rho/E_2}$, laminate $([0^\circ/90^\circ/90^\circ/0^\circ])$ grid 13×13 points, $a/h = 100$, $R/a = 10$

elastic shells. *International Journal of Engineering Science*, 23:319–330, 1985.

- [4] M. Touratier. An efficient standard plate theory. *International Journal of Engineering Science*, 29(8):901 â 916, 1991. Cited by: 1024.
- [5] J. N. Reddy. *Mechanics of laminated composite plates*. CRC Press, New York, 1997.
- [6] E. J. Kansa. Multiquadrics- a scattered data approximation scheme with applications to computational fluid dynamics. i: Surface approximations and partial derivative estimates. *Computers and Mathematics with Applications*, 19(8/9):127–145, 1990.

- [7] A. J. M. Ferreira. A formulation of the multiquadric radial basis function method for the analysis of laminated composite plates. *Composite Structures*, 59:385–392, 2003.
- [8] A. J. M. Ferreira, C. M. C. Roque, and P. A. L. S. Martins. Analysis of composite plates using higher-order shear deformation theory and a finite point formulation based on the multiquadric radial basis function method. *Composites: Part B*, 34:627–636, 2003.
- [9] E. Carrera. Developments, ideas, and evaluations based upon reissner’s mixed variational theorem in the modelling of multilayered plates and shells. *Applied Mechanics Reviews*, 54:301–329, 2001.
- [10] E. Carrera. Evaluation of layer-wise mixed theories for laminated plate analysis. *AIAA Journal*, (36):830–839, 1998.
- [11] Erasmo Carrera. Multilayered shell theories accounting for layerwise mixed description, part 1: Governing equations. *AIAA Journal*, 37(9):1107–1116, 1999.
- [12] Erasmo Carrera. Multilayered shell theories accounting for layerwise mixed description, part 2: Numerical evaluations. *AIAA Journal*, 37(9):1117–1124, 1999.
- [13] L.N. Trefethen. *Spectral Methods in MATLAB*. Software, Environments, and Tools. Society for Industrial and Applied Mathematics, 2000.
- [14] Maria Cinefra, S. Keshava Kumar, and Erasmo Carrera. Mitc9 shell elements based on rmvt and cuf for the analysis of laminated composite plates and shells. *Composite Structures*, 209:383 à 390, 2019. Cited by: 10.

		Method	R/a				
a/h			5	10	100	10^9	
[0°/90°/0°]	10	present (13 × 13)	7.0502	7.3025	7.3959	7.3978	
	10	present (17 × 17)	7.0502	7.3025	7.3959	7.3978	
	10	present (21 × 21)	7.0502	7.3025	7.3958	7.3978	
	10	HSDT [3]	6.7688	7.0325	7.1240	7.125	
	10	FSDT [3]	6.4253	6.6247	6.6923	6.6939	
	10	LW [12]	7.0834	7.3252	7.4087	7.4095	
	100	present (13 × 13)	1.0312	2.4003	4.2722	4.3062	
	100	present (17 × 17)	1.0312	2.4003	4.2722	4.3062	
	100	present (21 × 21)	1.0312	2.4003	4.2722	4.3062	
	100	HSDT [3]	1.0321	2.4099	4.3074	4.3420	
	100	FSDT [3]	1.0337	2.4109	4.3026	4.3370	
	100	LW [12]	1.0340	2.4120	4.3055	4.3400	
	[0°/90°/90°/0°]	10	present (13 × 13)	7.0084	7.2597	7.3525	7.3544
		10	present (17 × 17)	7.0084	7.2597	7.3525	7.3544
		10	present (21 × 21)	7.0084	7.2597	7.3525	7.3544
10		HSDT [3]	6.7865	7.0536	7.1464	7.1474	
10		FSDT [3]	6.3623	6.5595	6.6264	6.6280	
10		LW [12]	6.9953	7.2322	7.3139	7.3148	
100		present (13 × 13)	1.0255	2.3925	4.2712	4.3054	
100		present (17 × 17)	1.0255	2.3925	4.2712	4.3054	
100		present (21 × 21)	1.0255	2.3925	4.2713	4.3054	
100		HSDT [3]	1.0264	2.4024	4.3082	4.3430	
100		FSDT [3]	1.0279	2.4030	4.3021	4.3368	
100		LW [12]	1.0284	2.4048	4.3073	4.3420	

Table 2

Non-dimensional central deflection, $\bar{w} = w \frac{10^3 E_2 h^3}{P_0 a^4}$ variation with various number of grid points per unit length, N for different R/a ratios, for $R_1 = R_2$

a/h	Method	R/a			
		5	10	100	10^9
10	present (13 × 13)	11.8122	11.6430	11.5863	11.5857
	present (17 × 17)	11.8122	11.6430	11.5863	11.5857
	present (21 × 21)	11.8122	11.6430	11.5863	11.5857
	HSDT [3]	12.040	11.840	11.780	11.780
100	present (13 × 13)	31.1113	20.4229	15.2988	15.2381
	present (17 × 17)	31.1113	20.4229	15.2988	15.2381
	present (21 × 21)	31.1113	20.4229	15.2988	15.2381
	HSDT [3]	31.100	20.380	15.230	15.170

Table 3
Nondimensionalized fundamental frequencies of cross-ply laminated spherical shells,
 $\bar{\omega} = \omega \frac{a^2}{h} \sqrt{\rho/E_2}$, laminate ($[0^\circ/90^\circ/90^\circ/0^\circ]$)

a/h	Method	R/a			
		5	10	100	10^9
10	present (13 × 13)	11.7716	11.6030	11.5465	11.5459
	present (17 × 17)	11.7716	11.6030	11.5465	11.5459
	present (21 × 21)	11.7716	11.6030	11.5465	11.5459
	HSDT[3]	12.060	11.860	11.790	11.790
100	present (13 × 13)	31.0280	20.3899	15.2970	15.2368
	present (17 × 17)	31.0280	20.3899	15.2970	15.2368
	present (21 × 21)	31.0280	20.3899	15.2970	15.2368
	HSDT[3]	31.0398	20.350	15.240	15.170

Table 4
Nondimensionalized fundamental frequencies of cross-ply laminated spherical shells,
 $\bar{\omega} = \omega \frac{a^2}{h} \sqrt{\rho/E_2}$, laminate ($[0^\circ/90^\circ/0^\circ]$)

R/a	Method	[0/90/0]		[0/90/90/0]	
		$a/h = 100$	$a/h = 10$	$a/h = 100$	$a/h = 10$
5	present (13 × 13)	20.3373	11.5610	20.3747	11.6064
	present (17 × 17)	20.3373	11.5610	20.3747	11.6064
	present (21 × 21)	20.3373	11.5610	20.3747	11.6064
	FSDT [3]	20.332	12.207	20.361	12.267
	HSDT [3]	20.330	11.850	20.360	11.830
10	present (13 × 13)	16.6629	11.5497	16.6752	11.5909
	present (17 × 17)	16.6629	11.5497	16.6752	11.5909
	present (21 × 21)	16.6629	11.5497	16.6752	11.5909
	FSDT [3]	16.625	12.173	16.634	12.236
	HSDT [3]	16.620	11.800	16.630	11.790
100	present (13 × 13)	15.2517	11.5459	15.2532	11.5858
	present (17 × 17)	15.2517	11.5459	15.2532	11.5858
	present (21 × 21)	15.2517	11.5459	15.2532	11.5858
	FSDT [3]	15.198	12.163	15.199	12.227
	HSDT [3]	15.19	11.79	15.19	11.78
Plate	present (13 × 13)	15.2368	11.5459	15.2382	11.5857
	present (17 × 17)	15.2368	11.5459	15.2382	11.5857
	present (21 × 21)	15.2368	11.5459	15.2382	11.5857
	FSDT [3]	15.183	12.162	15.184	12.226
	HSDT [3]	15.170	11.790	15.170	11.780

Table 5

Nondimensionalized fundamental frequencies of cross-ply cylindrical shells, $\bar{\omega} = \omega \frac{a^2}{h} \sqrt{\rho/E_2}$